



<b>Title</b>	<b>decay of Cd129 and excited states in In129</b>
<b>Author(s)</b>	<b>Taprogge, J; Jungclaus, A; Grawe, H; Nishimura, S; Doornenbal, P; Lorusso, G; Simpson, G; Söderström, P; Sumikama, T; Xu, Z</b>
<b>Citation</b>	<b>Physical Review C, 2015, v. 91, article no. 054324</b>
<b>Issued Date</b>	<b>2015</b>
<b>URL</b>	<b><a href="http://hdl.handle.net/10722/214469">http://hdl.handle.net/10722/214469</a></b>
<b>Rights</b>	<b>Creative Commons: Attribution 3.0 Hong Kong License</b>

**$\beta$  decay of  $^{129}\text{Cd}$  and excited states in  $^{129}\text{In}$** 

J. Taprogge,<sup>1,2,3,\*</sup> A. Jungclaus,<sup>1</sup> H. Grawe,<sup>4</sup> S. Nishimura,<sup>3</sup> P. Doornenbal,<sup>3</sup> G. Lorusso,<sup>3,5,6</sup> G. S. Simpson,<sup>7</sup> P.-A. Söderström,<sup>3</sup> T. Sumikama,<sup>8</sup> Z. Y. Xu,<sup>9</sup> H. Baba,<sup>3</sup> F. Browne,<sup>3,10</sup> N. Fukuda,<sup>3</sup> R. Gernhäuser,<sup>11</sup> G. Gey,<sup>3,7,12</sup> N. Inabe,<sup>3</sup> T. Isobe,<sup>3</sup> H. S. Jung,<sup>13,†</sup> D. Kameda,<sup>3</sup> G. D. Kim,<sup>14</sup> Y.-K. Kim,<sup>14,15</sup> I. Kojouharov,<sup>4</sup> T. Kubo,<sup>3</sup> N. Kurz,<sup>4</sup> Y. K. Kwon,<sup>14</sup> Z. Li,<sup>16</sup> H. Sakurai,<sup>3,9</sup> H. Schaffner,<sup>4</sup> K. Steiger,<sup>11</sup> H. Suzuki,<sup>3</sup> H. Takeda,<sup>3</sup> Zs. Vajta,<sup>3,17</sup> H. Watanabe,<sup>3</sup> J. Wu,<sup>3,16</sup> A. Yagi,<sup>18</sup> K. Yoshinaga,<sup>19</sup> G. Benzoni,<sup>20</sup> S. Bönig,<sup>21</sup> K. Y. Chae,<sup>22</sup> L. Coraggio,<sup>23</sup> A. Covello,<sup>23,24</sup> J.-M. Daugas,<sup>25</sup> F. Drouet,<sup>7</sup> A. Gadea,<sup>26</sup> A. Gargano,<sup>23</sup> S. Ilieva,<sup>21</sup> F. G. Kondev,<sup>27</sup> T. Kröll,<sup>21</sup> G. J. Lane,<sup>28</sup> A. Montaner-Pizá,<sup>26</sup> K. Moschner,<sup>29</sup> D. Mücher,<sup>11</sup> F. Naqvi,<sup>30</sup> M. Niikura,<sup>9</sup> H. Nishibata,<sup>18</sup> A. Odahara,<sup>18</sup> R. Orlandi,<sup>31,32</sup> Z. Patel,<sup>6</sup> Zs. Podolyák,<sup>6</sup> and A. Wendt<sup>29</sup>

<sup>1</sup>*Instituto de Estructura de la Materia, CSIC, E-28006 Madrid, Spain*

<sup>2</sup>*Departamento de Física Teórica, Universidad Autónoma de Madrid, E-28049 Madrid, Spain*

<sup>3</sup>*RIKEN Nishina Center, RIKEN, 2-1 Hirosawa, Wako-shi, Saitama 351-0198, Japan*

<sup>4</sup>*GSI Helmholtzzentrum für Schwerionenforschung GmbH, 64291 Darmstadt, Germany*

<sup>5</sup>*National Physical Laboratory, NPL, Teddington, Middlesex TW11 0LW, United Kingdom*

<sup>6</sup>*Department of Physics, University of Surrey, Guildford GU2 7XH, United Kingdom*

<sup>7</sup>*LPSC, Université Joseph Fourier Grenoble 1, CNRS/IN2P3, Institut National Polytechnique de Grenoble, F-38026 Grenoble Cedex, France*

<sup>8</sup>*Department of Physics, Tohoku University, Aoba, Sendai, Miyagi 980-8578, Japan*

<sup>9</sup>*Department of Physics, University of Tokyo, Hongo 7-3-1, Bunkyo-ku, 113-0033 Tokyo, Japan*

<sup>10</sup>*School of Computing, Engineering and Mathematics, University of Brighton, Brighton BN2 4JG, United Kingdom*

<sup>11</sup>*Physik Department E12, Technische Universität München, D-85748 Garching, Germany*

<sup>12</sup>*Institut Laue-Langevin, B.P. 156, F-38042 Grenoble Cedex 9, France*

<sup>13</sup>*Department of Physics, Chung-Ang University, Seoul 156-756, Republic of Korea*

<sup>14</sup>*Rare Isotope Science Project, Institute for Basic Science, Daejeon 305-811, Republic of Korea*

<sup>15</sup>*Department of Nuclear Engineering, Hanyang University, Seoul 133-791, Republic of Korea*

<sup>16</sup>*School of Physics and State key Laboratory of Nuclear Physics and Technology, Peking University, Beijing 100871, China*

<sup>17</sup>*MTA Atomki, P.O. Box 51, Debrecen H-4001, Hungary*

<sup>18</sup>*Department of Physics, Osaka University, Machikaneyama-machi 1-1, Osaka 560-0043 Toyonaka, Japan*

<sup>19</sup>*Department of Physics, Faculty of Science and Technology, Tokyo University of Science, 2641 Yamazaki, Noda, Chiba, Japan*

<sup>20</sup>*INFN, Sezione di Milano, via Celoria 16, I-20133 Milano, Italy*

<sup>21</sup>*Institut für Kernphysik, Technische Universität Darmstadt, D-64289 Darmstadt, Germany*

<sup>22</sup>*Department of Physics, Sungkyunkwan University, Suwon 440-746, Republic of Korea*

<sup>23</sup>*Istituto Nazionale di Fisica Nucleare, Complesso Universitario di Monte S. Angelo, I-80126 Napoli, Italy*

<sup>24</sup>*Dipartimento di Fisica, Università di Napoli Federico II, Complesso Universitario di Monte S. Angelo, I-80126 Napoli, Italy*

<sup>25</sup>*CEA, DAM, DIF, 91297 Arpajon Cedex, France*

<sup>26</sup>*Instituto de Física Corpuscular, CSIC-Univ. of Valencia, E-46980 Paterna, Spain*

<sup>27</sup>*Nuclear Engineering Division, Argonne National Laboratory, Argonne, Illinois 60439, USA*

<sup>28</sup>*Department of Nuclear Physics, Research School of Physical Sciences and Engineering, Australian National University, Canberra, A.C.T 0200, Australia*

<sup>29</sup>*IKP, University of Cologne, D-50937 Cologne, Germany*

<sup>30</sup>*Wright Nuclear Structure Laboratory, Yale University, New Haven, Connecticut 06520-8120, USA*

<sup>31</sup>*Instituut voor Kern- en Stralingsfysica, K.U. Leuven, B-3001 Heverlee, Belgium*

<sup>32</sup>*Advanced Science Research Center, Japan Atomic Energy Agency, Tokai, Ibaraki, 319-1195, Japan*

(Received 19 January 2015; revised manuscript received 30 April 2015; published 26 May 2015)

The  $\beta$  decay of  $^{129}\text{Cd}$ , produced in the relativistic fission of a  $^{238}\text{U}$  beam, was experimentally studied at the RIBF facility at the RIKEN Nishina Center. From the  $\gamma$  radiation emitted after the  $\beta$  decays, a level scheme of  $^{129}\text{In}$  was established comprising 31 excited states and 69  $\gamma$ -ray transitions. The experimentally determined level energies are compared to state-of-the-art shell-model calculations. The half-lives of the two  $\beta$ -decaying states in  $^{129}\text{Cd}$  were deduced and the  $\beta$  feeding to excited states in  $^{129}\text{In}$  were analyzed. It is found that, as in most cases in the  $Z < 50$ ,  $N \leq 82$  region, both decays are dominated by the  $\nu 0g_{7/2} \rightarrow \pi 0g_{9/2}$  Gamow–Teller transition, although the contribution of first-forbidden transitions cannot be neglected.

DOI: 10.1103/PhysRevC.91.054324

PACS number(s): 23.20.Lv, 23.40.–s, 21.60.Cs, 27.60.+j

**I. INTRODUCTION**

The region around the doubly magic  $^{132}\text{Sn}$  is of particular interest for nuclear structure studies. With eight neutrons more than the last stable Sn isotope,  $^{132}\text{Sn}$  is the heaviest nucleus

\*Corresponding author: j.taprogge@csic.es

†Present address: Department of Physics, University of Notre Dame, Notre Dame, Indiana 46556, USA.

far from the valley of stability with both a closed proton and neutron shell currently available for study. Consequently, the nuclei in close proximity are a perfect test ground for nuclear models far from stability. Furthermore, the  $\beta$ -decay properties in the region below  $Z = 50$  have a crucial impact on calculations of the  $r$  process, one of the main processes responsible for the synthesis of the heavier elements in the universe. The relative abundances around the neutron shell closures are particularly sensitive to the  $\beta$ -decay half-lives of the  $r$ -process nuclei [1]. It is therefore of major interest to have models which can predict the half-lives of nuclei in the experimentally inaccessible regions with high accuracy. One of the questions related to that is if and how much first-forbidden (ff)  $\beta$  decays contribute in the region around  $N = 82$ . Different theoretical approaches led to different conclusions regarding this point in the past [2–4].

In a recent experiment at the RIKEN Nishina Center several nuclei around  $^{132}\text{Sn}$  were produced, taking advantage of the high intensity of the primary uranium beam available at that facility. First results from this experiment have already been presented for ms and  $\mu\text{s}$  isomeric states in  $^{129}\text{Cd}$  [5] and  $^{136,138}\text{Sn}$  [6] as well as for the  $\beta$  decays of  $^{131,132}\text{Cd}$  [7] populating excited states in  $^{131}\text{In}$ . In the present work, we report on the  $\beta$  decay of  $^{129}\text{Cd}$ , which has two proton holes and one neutron hole with respect to the  $^{132}\text{Sn}$  core. This study includes the half-lives of the  $\beta$ -decaying states and the structure of the daughter nucleus  $^{129}\text{In}$ .

Prior to this work two  $\beta$ -decaying states in  $^{129}\text{Cd}$  with half-lives of 104 (6) and 242 (8) ms, respectively, have been reported [8–11]. While the longer half-life was associated with the proposed  $11/2^-$  ground state, the shorter half-life was assigned to a  $3/2^+$   $\beta$ -decaying isomer [9,10]. Recently, the work by Yordanov *et al.* confirmed the existence of the  $3/2^+$  and  $11/2^-$  long-lived states in  $^{129}\text{Cd}$  via laser spectroscopy [12]. However, experimental information on the order of those two states is still missing. In Ref. [5] we reported the first experimental information about  $\gamma$ -decaying excited states in  $^{129}\text{Cd}$  by observing the decay of an isomeric state with a half-life of  $T_{1/2} = 3.6$  (2) ms and a tentative spin and parity assignment of  $(21/2^+)$ . The shell-model calculations performed in that work indeed suggest that the  $11/2^-$  state is the ground state with the  $3/2^+$  state placed at an excitation energy of 287 keV.

More information is available for  $^{129}\text{In}$ . Besides the  $9/2^+$  ground state, a  $\beta$ -decaying  $1/2^-$  isomer has been reported [13]. The excitation energy of this  $1/2^-$  state has been fixed to be 459 (5) keV in a recent mass measurement [14]. Furthermore Fogelberg *et al.* have shown evidence of two long-lived high-spin states with spins of  $(29/2^+)$  and  $(23/2^-)$  for which half-lives of 110 and 700 ms, respectively, were measured [15]. The  $(23/2^-)$  state was identified as an  $\beta$ -decaying isomer and placed at an excitation energy of 1630 (56) keV in Ref. [16]. In addition a  $17/2^-$  isomeric state with a half-life of 8.5 (5)  $\mu\text{s}$  was observed by Genevey *et al.* at an excitation energy of 1688 keV, decaying via a cascade to the  $9/2^+$  ground state [17]. Finally, more than 50  $\gamma$ -ray transitions were observed following the  $\beta$  decay of  $^{129}\text{Cd}$  in the experiments performed at the CERN On-Line Isotope Mass Separator (ISOLDE) facility [11,18]. A level scheme

of  $^{129}\text{In}$  including 18 of these transitions was presented in Ref. [11].

## II. EXPERIMENTAL METHOD

The experiment was carried out at the Radioactive Isotope Beam Factory (RIBF) at the RIKEN Nishina Center (Japan). The ions of interest were produced via in-flight fission of a  $^{238}\text{U}$  primary beam with an energy of 345 MeV/u which impinged on a 3-mm-thick Be production target. Employing the fragment separator BigRIPS [19], the ions of interest were separated and identified on an event-by-event basis. The charge  $Z$  and the mass-to-charge ratio  $A/q$  were determined by measuring the time of flight (ToF), the energy loss  $\Delta E$ , and the magnetic rigidity  $B\rho$  with the BigRIPS detectors. A more detailed description of the separation and identification procedures can be found in Ref. [20].

In total,  $3.2 \times 10^6$   $^{129}\text{Cd}$  ions were identified and transported through the ZeroDegree spectrometer to the final focal plane where an active stopper was placed. The active stopper, called the wide-range active silicon strip stopper array for  $\beta$  and ion detection (WAS3ABi) comprises eight double-sided Si strip detectors (DSSSD) with each of them having an active area of  $60 \times 40$  mm<sup>2</sup> and a segmentation into 60 vertical by 40 horizontal strips [21]. The DSSSDs have a thickness of 1 mm each, are closely packed behind each other, and are placed at the center of the EUROBALL-RIKEN Cluster Array (EURICA) [22], an array of 12 large-volume germanium cluster detectors of the former EUROBALL array [23]. The  $^{129}\text{Cd}$  ions were implanted in WAS3ABi and by means of the position- and time-difference correlated offline to subsequent decay events observed in WAS3ABi. The maximum time difference to correlate decay and implantation events was chosen according to the half-life of the parent nucleus, in this case  $^{129}\text{Cd}$ , and the application. For example, for investigating the  $\gamma$  rays following the decay of  $^{129}\text{Cd}$  the maximum correlation time was set to 450 ms, while for the half-life analysis a longer correlation time was necessary.

To improve the efficiency for higher-energy  $\gamma$  rays an add-back procedure was applied, summing the energies of two neighboring crystals if their energy sum is above 100 keV and if the signals are recorded within a prompt-coincidence time window of 500 ns. The resulting absolute efficiency of the germanium array for a  $\gamma$  ray at 1 MeV (4 MeV) was determined to be 8.5 (4)% [2.9 (2)%].

## III. EXPERIMENTAL RESULTS

The germanium add-back spectrum recorded in coincidence with the first decay observed in WAS3ABi within a maximum correlation time of 450 ms, requiring that implantation and decay occurred in the same DSSSD and with a maximum position difference of 1 mm in the  $x$  and  $y$  directions, is shown in Fig. 1 for the energy range up to 5 MeV. While most observed transitions can be assigned to the  $\beta$  decay of  $^{129}\text{Cd}$  to  $^{129}\text{In}$ , several peaks can be attributed to other decays.

Transitions belonging to the decay of the daughter nucleus  $^{129}\text{In}$  (%) are observed, populating levels in  $^{129}\text{Sn}$ . Due to the limited efficiency for detecting  $\beta$  electrons the decay of

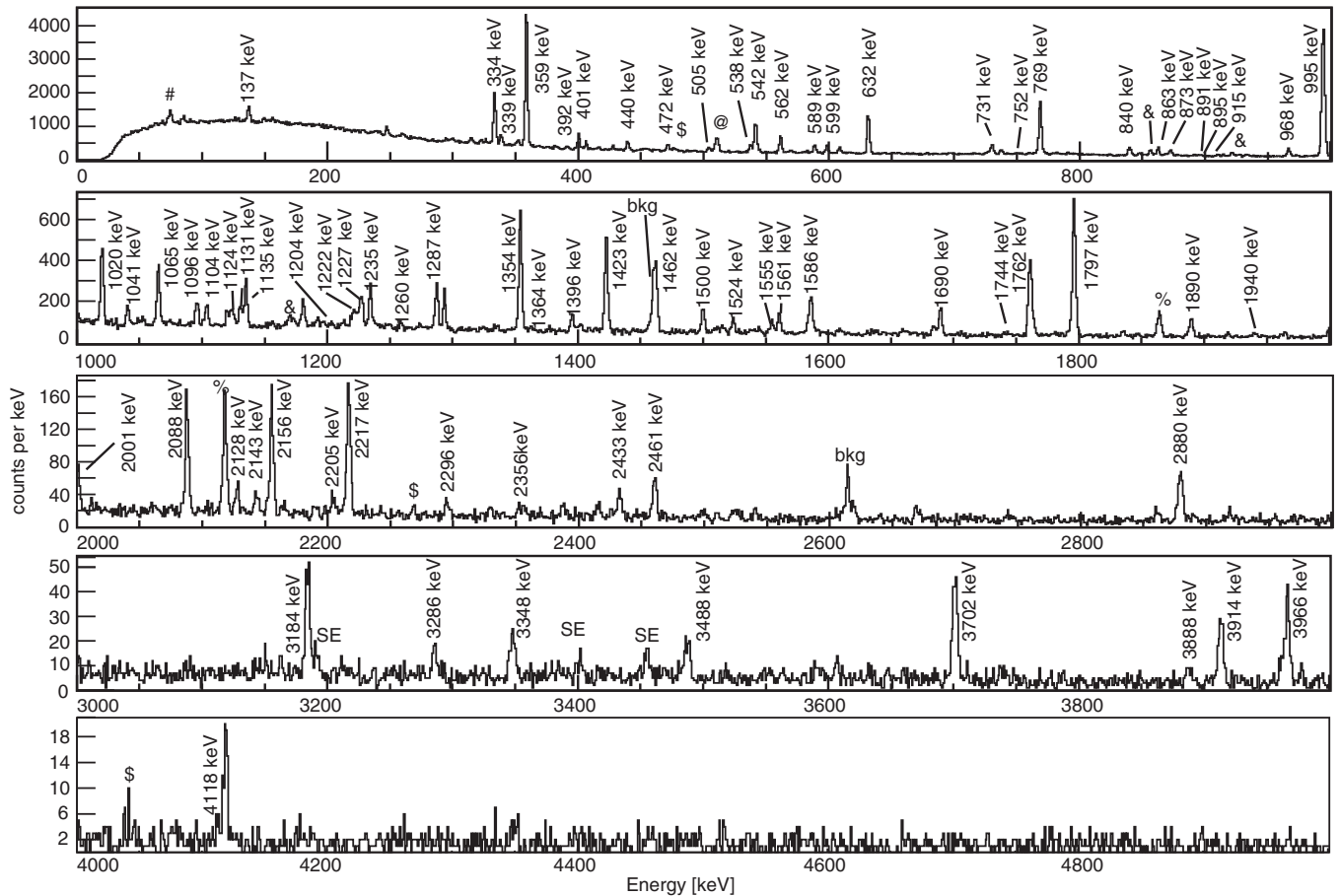


FIG. 1. Germanium add-back spectrum recorded in coincidence with the first  $\beta$  decay observed in WAS3ABi within 450 ms after the implantation of a  $^{129}\text{Cd}$  ion and requiring that the implantation and the decay occurred in the same DSSSD and with a maximum position difference of 1 mm in the horizontal and vertical directions. The transitions labeled with symbols correspond to known transitions in  $^{129}\text{Sn}$  (%), populated in the  $\beta$  decay of the daughter nucleus  $^{129}\text{In}$ , in  $^{128}\text{In}$  (&), populated after  $\beta$ -delayed neutron emission from  $^{129}\text{Cd}$  or the decay of  $^{128}\text{Cd}$  (see text for details), in  $^{131}\text{Sn}$  (#) and  $^{132}\text{Sn}$  (\$), through the false correlation of  $\beta$  decays of  $^{131}\text{In}$  and  $^{132}\text{In}$  to the implanted  $^{129}\text{Cd}$  ions and the annihilation of positrons produced in the pair creation in the germanium detectors (@). Single-escape peaks have been marked with (SE) and peaks arising from room background with (bkg).

$^{129}\text{Cd}$  may escape observation and the first detected decay after the implantation is then the decay of the daughter nucleus. In addition to that, transitions in  $^{128}\text{In}$  (&) are present in the spectrum, which are either populated through  $\beta$ -delayed neutron emission of  $^{129}\text{Cd}$  or due to reactions occurring in the material placed in the beamline, e.g., detectors or degraders, after the ion identification, meaning that  $^{128}\text{Cd}$  not  $^{129}\text{Cd}$  was implanted. The peak at 511 keV (@) arises from the annihilation of positrons which have been created in pair production of high-energy  $\gamma$  rays. On top of that we observe several peaks which have been identified as single-escape peaks (SE) from high-energy transitions where one 511 keV  $\gamma$  ray escapes the detector after pair production.

In addition to the contaminations mentioned above, which can be correlated with the implanted  $^{129}\text{Cd}$  ions, several peaks can be assigned to strong transitions from other decays, e.g., transitions in  $^{131}\text{Sn}$  (#) and  $^{132}\text{Sn}$  (\$) emitted after the  $\beta$  decay of  $^{131}\text{In}$  and  $^{132}\text{In}$ , respectively. The nuclei  $^{131}\text{In}$  and  $^{132}\text{In}$  have been created with a much higher production yield than most of the other reaction channels and false correlations of

decay and implantation events can occur when the decay of those nuclei is detected in close proximity to the implantation position of the ion of interest. Those contamination lines are observed in most of the germanium spectra recorded after the decay of the individual nuclei produced in this experiment. Peaks arising from room background (bkg) are also observed and marked in Fig. 1.

### A. The level scheme of $^{129}\text{In}$

The energies and relative intensities of all  $\gamma$  rays which have been associated with the  $\beta$  decay of  $^{129}\text{Cd}$  to  $^{129}\text{In}$  are listed in Table I. Most of these 78 transitions have been placed in a level scheme taking into account information obtained from  $\gamma$ - $\gamma$  coincidence spectra and relative intensities. Coincidence spectra with short (500 ns) and long (100  $\mu\text{s}$ ) coincidence time windows have been investigated in detail for each transition and this piece of information was sufficient in most of the cases to fix the placement of the transitions in the level scheme of  $^{129}\text{In}$ . The placement of the transitions and



TABLE I. List of  $\gamma$  rays observed in the  $\beta$  decay of  $^{129}\text{Cd}$  to  $^{129}\text{In}$  with their energies, relative  $\gamma$  intensities, and the energies, spins, and parities of the initial and final states. The literature values of the relative intensities are taken from Ref. [11]. Any  $\gamma$  rays not placed in the level scheme shown in Fig. 3 are marked by an asterisk. The absolute intensity of the 995.1-keV-transition per decay of  $^{129}\text{Cd}$  is 33 (2)%. Assuming that 49 (4)% of all  $^{129}\text{Cd}$  decays proceed from the  $11/2^-$  state (see Sec. IV), absolute intensities of 63 (6)% and 4 (1)% are obtained for decays of the  $11/2^-$  and  $3/2^+$  states in  $^{129}\text{Cd}$ , respectively.

$E_\gamma$ [keV]	$I_\gamma$ [%]	$I_\gamma^{\text{lit}}$ [%]	$E_i$	$E_f$	$J_i^\pi$	$J_f^\pi$	$E_\gamma$ [keV]	$I_\gamma$ [%]	$I_\gamma^{\text{lit}}$ [%]	$E_i$	$E_f$	$J_i^\pi$	$J_f^\pi$
137.2	4.7(6) <sup>a</sup>		1220	1083	(5/2 <sup>-</sup> )	(3/2 <sup>-</sup> )	1287.3	7.0(7)		3348	2060	(5/2 <sup>+</sup> )	
334.1	19.9(12)	13.0	1688	1354	17/2 <sup>-</sup>	13/2 <sup>+</sup>	1354.2	20.5(12)	21.0	1354	0	13/2 <sup>+</sup>	9/2 <sup>+</sup>
339.1	6.5(7)	6.0	1693	1354		13/2 <sup>+</sup>	1363.6	1.0(5)		2447	1083		
358.9	57.4(30)	50.0	1354	995	13/2 <sup>+</sup>	11/2 <sup>+</sup>	1395.9*	3.0(15)					
391.7	1.4(7)		2085	1693			1422.9	16.9(10)	20.0	3184	1762	(5/2 <sup>+</sup> )	
400.8	6.3(6)	7.0	1621	1220		(5/2 <sup>-</sup> )	1457.0	1.4(1.2)		3150	1693	(13/2 <sup>-</sup> )	
439.7	2.7(3)	4.0	2060	1621			1462.3	12.2(12)	11.0	3150	1688	(13/2 <sup>-</sup> )	17/2 <sup>-</sup>
471.9	1.5(8)		1555	1083		(3/2 <sup>-</sup> )	1500.2*	4.4(5)					
504.5*	2.1(2)						1524.1	2.3(4)		3971	2447		
537.9	2.8(8)	2.0	1621	1083		(3/2 <sup>-</sup> )	1555.2	1.3(4)	5.0	1555	0		9/2 <sup>+</sup>
542.0	14.5(10)	11.0	1762	1220		(5/2 <sup>-</sup> )	1560.9*	2.7(11)	5.0				
561.8	8.5(8)	8.0	3150	2589	(13/2 <sup>-</sup> )		1586.2	8.3(8)	12.0	3348	1762	(5/2 <sup>+</sup> )	
589.1	3.2(4)	5.2	3150	2561	(13/2 <sup>-</sup> )		1689.9*	4.5(5)	6.0				
599.2	2.8(4)		3150	2551	(13/2 <sup>-</sup> )		1744.4	1.2(6)		3888	2143		
631.9	21.0(12)	30.0	1083	451	(3/2 <sup>-</sup> )	1/2 <sup>-</sup>	1761.6	16.4(12)	19.0	1762	0		9/2 <sup>+</sup>
731.0	6.2(7)	8.5	2085	1354		13/2 <sup>+</sup>	1796.5	26.4(15)	32.0	3150	1354	(13/2 <sup>-</sup> )	13/2 <sup>+</sup>
752.0	1.4(12)		3184	2433	(5/2 <sup>+</sup> )		1890.0*	5.0(6)					
769.2	43.8(40)		1220	451	(5/2 <sup>-</sup> )	1/2 <sup>-</sup>	1940.3	0.6(4)		3702	1762		
840.2	10.8(9)	6.0	2060	1220		(5/2 <sup>-</sup> )	2001.1*	5.3(12)					
863.1	3.8(4)	5.5	2551	1688		17/2 <sup>-</sup>	2088.0	8.1(9)	5.5	2088	0		9/2 <sup>+</sup>
873.0	3.6(5)		2561	1688		17/2 <sup>-</sup>	2127.6	1.4(7)		3888	2143		
891.0	1.4(12)		2447	1555			2143.4	1.4(7)		2143	0		9/2 <sup>+</sup>
895.0	1.4(12)		2589	1693			2155.6	6.4(8)		3150	995	(13/2 <sup>-</sup> )	11/2 <sup>+</sup>
915.0	1.4(12)		3348	2433	(5/2 <sup>+</sup> )		2204.8	0.6(4)		3966	1762		
967.6	6.2(7)		3184	2217	(5/2 <sup>+</sup> )		2216.8	7.5(9)	8.0	2217	0		9/2 <sup>+</sup>
995.1	100.0(51)	100.0	995	0	11/2 <sup>+</sup>	9/2 <sup>+</sup>	2295.6*	1.3(4)					
1020.1	10.1(8)	8.5	2015	995		11/2 <sup>+</sup>	2356.0	1.5(7)		4118	1762		
1040.6	2.3(5)		3184	2143	(5/2 <sup>+</sup> )		2433.4	5.3(6)		2433	0		9/2 <sup>+</sup>
1065.4	8.5(7)	8.0	3150	2085	(13/2 <sup>-</sup> )		2460.9	3.8(8)	6.0	4082	1621		
1096.0	6.7(7)		3184	2088	(5/2 <sup>+</sup> )		2880.2	4.3(10)	2.5	4082	1220		(5/2 <sup>-</sup> )
1103.8*	2.5(13)	5.0					3184.4	4.0(7)	3.0	3184	0	(5/2 <sup>+</sup> )	9/2 <sup>+</sup>
1124.1	2.5(13)		3184	2060	(5/2 <sup>+</sup> )		3286.1	1.3(4)		3286	0		9/2 <sup>+</sup>
1130.6	3.4(9)		3348	2217	(5/2 <sup>+</sup> )		3348.0	3.0(10)	4.0	3348	0	(5/2 <sup>+</sup> )	9/2 <sup>+</sup>
1135.2	6.8(7)		3150	2015	(13/2 <sup>-</sup> )		3487.7	1.4(6)	1.0	3488	0		9/2 <sup>+</sup>
1203.5	1.4(12)		3348	2143	(5/2 <sup>+</sup> )		3701.9	4.7(17)	6.0	3702	0		9/2 <sup>+</sup>
1221.6	6.3(9)		2217	995		11/2 <sup>+</sup>	3888.4	1.1(7)	2.0	3888	0		9/2 <sup>+</sup>
1227.3	3.6(27)		2447	1220		(5/2 <sup>-</sup> )	3913.8	2.7(5)	3.0	3914	0		9/2 <sup>+</sup>
1234.6	7.7(11)	5.0	2589	1354		13/2 <sup>+</sup>	3966.4	5.0(12)	4.0	3966	0		9/2 <sup>+</sup>
1259.6	1.4(5)		3348	2088	(5/2 <sup>+</sup> )		4118.3	1.7(5)	2.0	4118	0		9/2 <sup>+</sup>

<sup>a</sup>Intensity corrected for internal conversion assuming an  $M1$  transition.

the establishment of new levels is discussed in detail in the following.

### 1. Excited states feeding the 11/2<sup>+</sup>, 13/2<sup>+</sup>, and 17/2<sup>-</sup> levels

The decay of the 17/2<sup>-</sup>,  $E_x = 1688$  keV isomer in  $^{129}\text{In}$  is firmly established [17] and was used as a starting point to place the  $\gamma$  rays observed in this experiment into a level scheme. The four transitions with energies of 334.1, 358.9, 995.1, and 1354.2 keV, reported by Genevey *et al.* [17], are also observed in the present experiment. The information

obtained from coincidence spectra agrees with the previously proposed level scheme. Another very strong transition with an energy of 1796.5 keV is observed in prompt coincidence with only the 358.9, 995.1, and 1354.2 keV transitions [(see Fig. 2(a)]. A placement on top of the 13/2<sup>+</sup> level at 1354 keV, as suggested by Arndt *et al.* [11], is therefore in agreement with our experimental information, resulting in a level at 3150 keV. This level is also deexcited via a transition of 2155.6 keV, which is only observed in coincidence with the 995.1 keV transition [Fig. 2(b)]. In addition we observe two  $\gamma$  rays with energies of 1020.1 and 1135.2 keV in coincidence with each

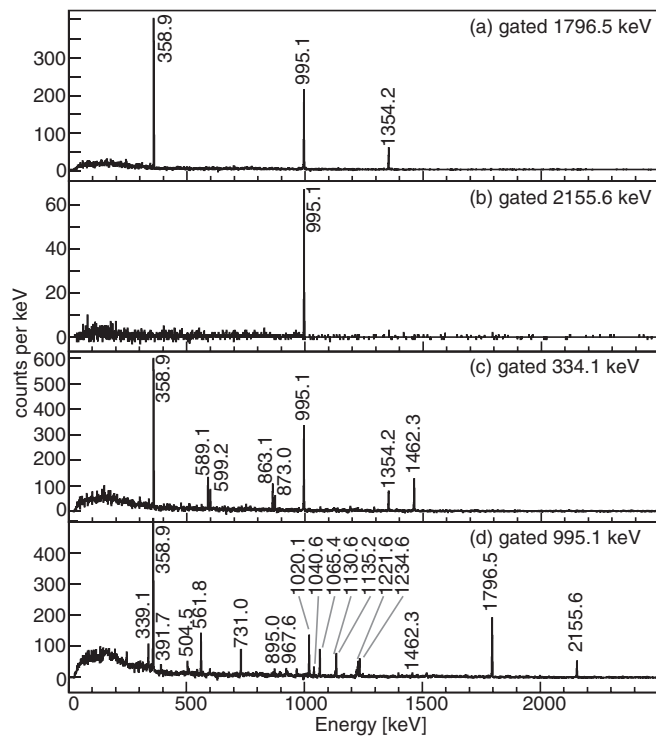


FIG. 2. The  $\gamma$ -ray spectra in (a) prompt coincidence with the the 1796.5 keV transition, (b) prompt coincidence with the 2155.6 keV transition, (c) coincidence (without time condition) with the 334.1 keV transition, and (d) prompt coincidence with the 995.1 keV transition.

other and with the 995.1 keV transition. From the coincidence information the only possible placement is on top of the 995 keV level, depopulating also the level at 3150 keV. The order within the cascade is fixed by the intensities of the two transitions.

Several other transitions (339.1, 391.7, 561.8, 731.0, 895.0, 1065.4, 1234.6, and 1457.0 keV) are observed in coincidence with the 358.9, 995.1, and 1354.2 keV transitions [see Figs. 2(c) and 2(d)] and can be placed in the level scheme as several cascades starting from the level at 3150 keV and ending in the 1354 keV level. The order of those cascades, as presented in Fig. 3, is fixed by the coincidence information and especially by the fact that  $\beta$  feeding is observed to all three levels at 1693, 2085, and 2589 keV.

Arndt *et al.* [11] suggested the placement of the 1462 keV transition on top of the  $17/2^-$   $\mu\text{s}$  isomeric state. We agree with this placement since the 1462.3 keV  $\gamma$  ray is observed in delayed coincidence with the 334.1 keV transition, see Fig. 2(c), and also with the 358.9, 995.1, and 1354.2 keV transitions. According to the coincidence information two more cascades can be placed on top of the  $17/2^-$  isomeric state. The first one comprises of the transitions with energies of 599.2 and 863.1 keV and the second the 589.1 and 873.0 keV transitions. Since the energy sum of both cascades is 1462 keV this suggests that they are in parallel to the 1462.3 keV transition. Due to the fact that the relative intensities of the transitions forming the cascades agree within the uncertainties their order cannot be determined.

Another three transitions are observed in prompt coincidence with only the 995.1 keV transition, having energies

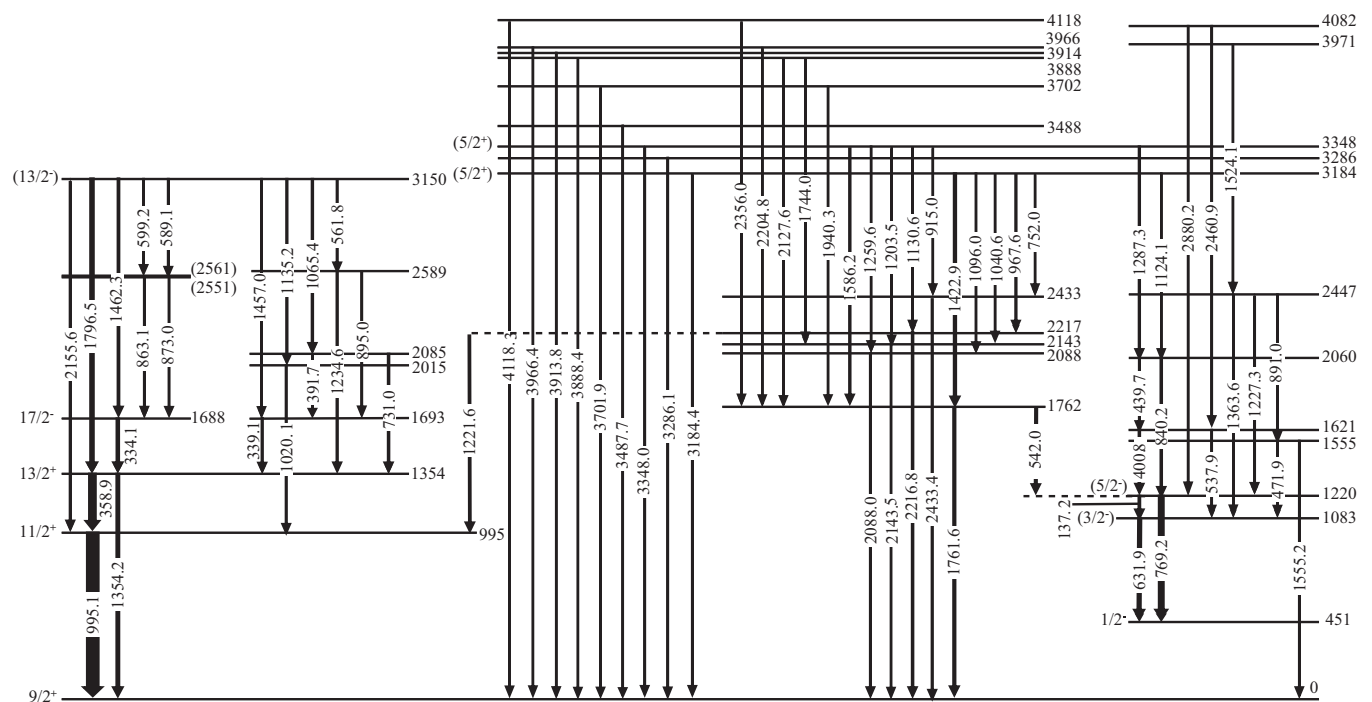


FIG. 3. Proposed level scheme of  $^{129}\text{In}$  established based on the intensities of and the coincidence relations between  $\gamma$  rays emitted following the  $\beta$  decay of  $^{129}\text{Cd}$ .

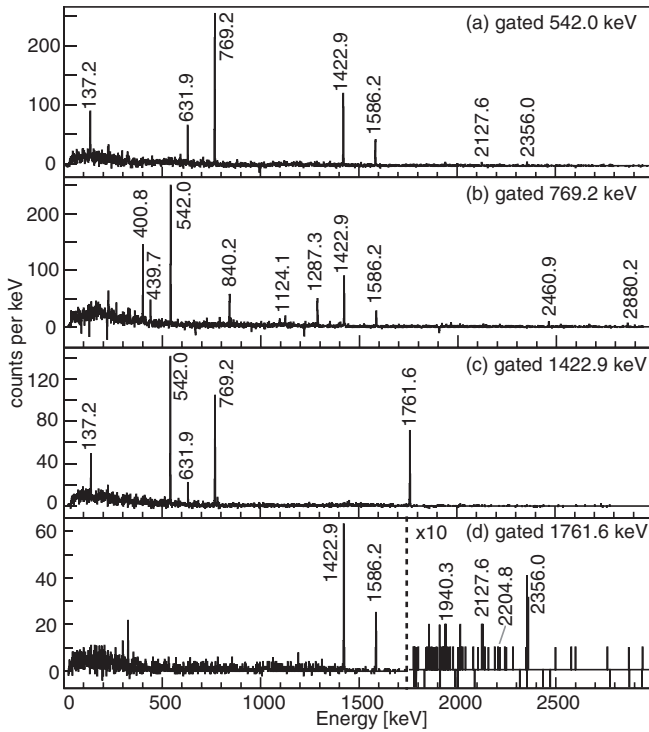


FIG. 4. The  $\gamma$ -ray spectra in prompt coincidence with (a) the 542.0 keV transition, (b) the 769.2 keV transition, (c) the 1422.9 keV transition, and (d) the 1761.6 keV transition.

of 967.6, 1130.6, and 1221.6 keV. Adding the fact that the 967.6 and 1130.6 keV transitions are seen in coincidence with a  $\gamma$  ray of 2216.8 keV fixes their placement in the level scheme establishing two new levels at 2217 and 3348 keV and confirming the one at 3184 keV proposed in Ref. [11].

### 2. The 3184, 3348, 3888, and 4118 keV levels

In the current experiment two  $\gamma$  rays with energies of 3184.4 and 3348.0 keV are observed and are placed as transitions to the ground state from the two levels established in the last section. By using the information from the  $\gamma$ - $\gamma$  coincidences, several cascades can be identified which have sum energies of either 3184 or 3348 keV. Placing those cascades establishes four new levels with energies of 1762, 2088, 2143, and 2433 keV. Note that the coincidence relation of the 1761.6 with the 1422.9 (see Fig. 4) and 1586.2 keV transitions, respectively, makes a placement of those transitions as proposed by Arndt *et al.* [11] very unlikely. Considering the experimental information, those two transitions are placed on top of the 1762 keV level, thus depopulating the levels at 3184 and 3348 keV, respectively.

The two  $\gamma$  rays with energies of 2356.0 and 2127.6 keV are placed on top of the 1762 keV level based on their prompt coincidences with solely the 1761.6 keV transition, thus establishing two new levels at 3888 and 4118 keV. The observation of transitions with energies of 3888.4 and 4118.3 keV suggests that those levels have a decay branch directly to the ground state. Furthermore we observe several other high-energy transitions in the range from 3 to 4 MeV which are placed as ground-state transitions (3487.7, 3701.9,

3913.8, and 3966.4 keV). Note that the levels at 3702 and 3966 keV also decay via a  $\gamma$  transition to the 1762 keV level.

### 3. The position of the $1/2^-$ $\beta$ -decaying isomer

Taking into account the relative intensities and coincidence information of the 137.2, 631.9, and 769.2 keV transitions, the placement of those on top of the  $1/2^-$   $\beta$ -decaying isomer is suggested and can be fixed by using the additional coincidence information obtained for the 542.0 keV transition [see Fig. 4(a)]. As an additional example, the  $\gamma$ - $\gamma$  coincidence spectrum of the 769.2 keV transition is shown in Fig. 4(b). The proposed placement is shown in the level scheme in Fig. 3, fixing the energy of the  $1/2^-$   $\beta$ -decaying isomer from a network of  $\gamma$  transitions. The excitation energy of 451 (1) keV is slightly smaller as compared to the value of 459 (5) keV obtained from the mass measurements reported in Ref. [14].

Based upon the information of  $\gamma$ - $\gamma$  coincidences, the 400.8, 439.7, 471.9, 537.9, 840.2, 891.0, 1124.1, 1227.3, 1287.3, 1363.6, 1524.1, 2460.9, and 2880.2 keV transitions are placed on top of the 1083 and 1220 keV states, establishing several new levels and especially two new states at 3971 and 4082 keV. For the latter two levels no direct decay branches to either the  $1/2^-$   $\beta$ -decaying isomer or the  $9/2^+$  ground state have been observed.

Summarizing the obtained results for the  $\beta$  decay to  $^{129}\text{In}$ , from the 78 observed gamma-ray transitions 69 could be placed in the level scheme presented in Fig. 3. The placement of the remaining transitions is not possible based upon the available experimental data, especially because they are not observed in coincidence with any other transition. The nine transitions which could not be placed in the level scheme are marked with an (\*) in Table I.

### B. $\beta$ -decay half-lives

In order to determine the half-lives of the two  $\beta$ -decaying states of  $^{129}\text{Cd}$ , the time distribution of all decays associated with the implanted  $^{129}\text{Cd}$  ions was inspected. Surprisingly, besides the very-short-lived component with a half-life of 3.6 (2) ms [5] this curve shows no evidence for the presence of two significantly different half-life components associated with the decay of the two  $\beta$ -decaying states in  $^{129}\text{Cd}$ , as expected considering the previously reported values of 242 (8) and 104 (6) ms [8–11]. The total decay curve was then fit with a function considering the ms isomeric state and two different parent half-lives and the known half-lives of the  $9/2^+$  and  $1/2^-$   $\beta$ -decaying states, 611 (5) ms and 1.23 (3) s, respectively, in the  $^{129}\text{In}$  daughter [24]. Independent of the assumed relative population of the two  $\beta$ -decaying states in  $^{129}\text{Cd}$ , the fit procedure always led to identical half-lives for the two components. Therefore, the decay curve was finally fit with a fit function  $f(x)$  considering only one half-life for the  $^{129}\text{Cd}$  decay (besides the ms isomer and the daughter decays) and a value of  $T_{1/2} = 154$  (8) ms was obtained. The quality of this fit is demonstrated in Fig. 5, which shows the difference between the experimental decay curve and the fit function  $f(x)$  normalized to the latter. For comparison we also include the fit obtained with a fit function  $g(x)$  including two different components in the decay of  $^{129}\text{Cd}$  with half-lives of 242 and

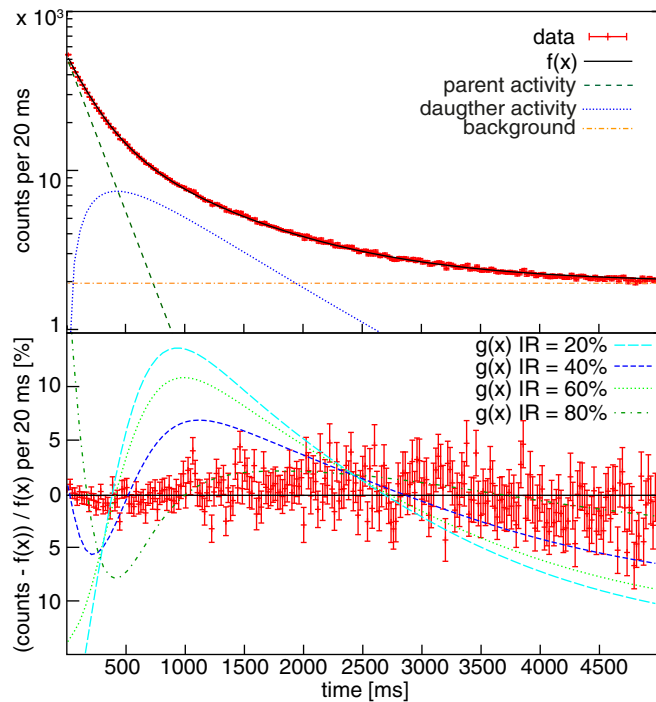


FIG. 5. (Color online) (top) Time distribution of all decays correlated to the implanted  $^{129}\text{Cd}$  ions and fit to the data with the fit function  $f(x)$  (see text for details). (bottom) Comparison between fits obtained with the fit function  $g(x)$ , which considers two  $\beta$ -decaying states in  $^{129}\text{Cd}$  with half-lives of 242 and 104 ms corresponding to the literature values, and the data. “IR” refers to the relative population of the 104-ms-half-life component (see text for details).

104 ms corresponding to the literature values [8–11]. Again the relative population of the two decaying states has been varied. The experimental data clearly exclude the existence of two decay components with the quoted half-lives.

An alternative way to try to disentangle the two different decay components originating from the  $11/2^-$  and  $3/2^+$  states in  $^{129}\text{Cd}$  is provided by the  $\beta$ - $\gamma$ -gating method. Decay curves were produced for the time difference between the implantation and the observation of a  $\beta$  decay in coincidence with a  $\gamma$  ray in the daughter nucleus. These decay curves should solely include the activity of the parent nucleus and can be fit with a single-exponential decay curve and a constant background. Via the selection of specific transitions in the daughter nucleus it is possible to produce decay curves showing the activity of only the  $3/2^+$  or the  $11/2^-$   $\beta$ -decaying state of  $^{129}\text{Cd}$ . Based on the level scheme obtained in the present work, the 358.9, 995.1, 1354.2, 1796.5, and 2155.6 keV transitions, mainly populated from the state at 3150 keV, are assumed to follow the decay of the  $11/2^-$   $\beta$ -decaying state, while the decay curves gated on the 1422.9 and 1586.2 keV transitions, depopulating the states at 3184 and 3384 keV, respectively, reflect most likely the activity of the  $3/2^+$  state in  $^{129}\text{Cd}$  (see Sec. IV for details).

For the decay of the  $11/2^-$  state, the half-life was deduced for each  $\gamma$  transition listed above individually and from the summed time distribution. Figure 6(a) shows the sum of the individual decay curves and the corresponding fit with a single-

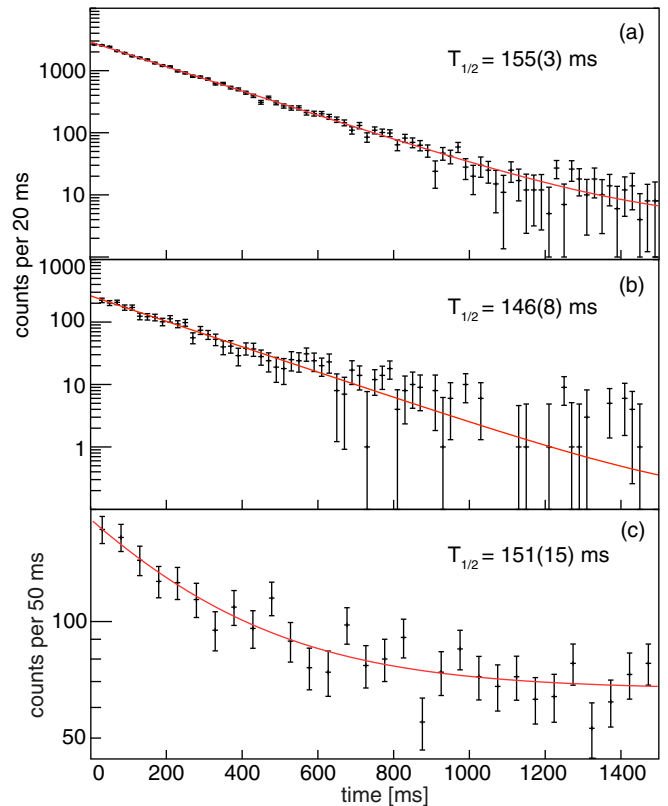


FIG. 6. (Color online) Summed time distributions for the decays of the two  $\beta$ -decaying states in  $^{129}\text{Cd}$  in coincidence with (a) the 358.9, 995.1, 1354.2, 1796.5, and 2155.6 keV transitions, and (b) the 1422.9 and 1586.2 keV transitions in the daughter nucleus  $^{129}\text{In}$ . The fit with a single-exponential decay function is shown in red. (c) The time distribution of all decays following the decay of the ms isomer in  $^{129}\text{Cd}$  (see text for details) and fit to the data with the fit function accounting for the activity of the  $11/2^-$  state in  $^{129}\text{Cd}$ , the activities of the two  $\beta$ -decaying states in the daughter nucleus  $^{129}\text{In}$ , and a constant background.

exponential decay function and a constant background. The fit results in a half-life of 155 (3) ms for the  $11/2^-$   $\beta$ -decaying state. None of the fits to the decay curves gated on individual transitions showed a significant deviation and the weighted mean half-life from those is 154 (2) ms, in good agreement with the value obtained for the summed time distribution. The sum of the time distributions obtained with gate on the 1422.9 and 1586.2 keV transitions is shown in Fig. 6(b) with the fitted half-life for the  $3/2^+$   $\beta$ -decaying state being 146 (8) ms. Thus, in our analysis, the half-lives of the two  $\beta$ -decaying states in  $^{129}\text{Cd}$  agree within the experimental uncertainties.

Finally, there is one more independent approach to determine the half-life of the  $11/2^-$  state. The  $^{129}\text{Cd}$  ( $21/2^+$ ),  $T_{1/2} = 3.6$  (2) ms isomer reported in Ref. [5] decays via the emission of  $\gamma$  rays with energies of 353, 406, 1181, and 1587 keV to the  $11/2^-$  state. A spectrum was filled with the difference between the time of the observation of one of these transitions and the time of the next decay event. In the fit of this time-difference spectrum, shown in Fig. 6(c), only the half-life of the  $11/2^-$  state in  $^{129}\text{Cd}$  has to be considered besides the



half-lives of the two  $\beta$ -decaying states in the daughter nucleus  $^{129}\text{In}$ . In this way a half-life of 151 (15) ms was extracted for the  $11/2^-$  state in  $^{129}\text{Cd}$ , in nice agreement with the values quoted above.

#### IV. THE DECAY $^{129}\text{Cd} \rightarrow ^{129}\text{In}$

While some feeding is observed to the low-lying levels up to approximately 2 MeV, the major part of the  $\beta$  decay of  $^{129}\text{Cd}$  proceeds to the three excited states at energies of 3150, 3184, and 3348 keV. In order to determine the character of these decays, the absolute intensities of the  $\beta$  feeding to individual states has to be determined. In a first step the absolute intensities of all observed  $\gamma$  rays were determined from a spectrum, taking into account not only the first, but all successive decays correlated with each implanted  $^{129}\text{Cd}$  ion within the first 4.5 s after the implantation. The number of decaying  $^{129}\text{Cd}$  ions was determined from the fit of the total decay curve discussed in the last section. In this way the number of decays is obtained in a direct way without the need to determine the  $\beta$  efficiency of the setup. The  $\beta$  feeding to each individual excited state is then obtained as the difference between the sum of the absolute intensities of the  $\gamma$  rays depopulating this state and the sum of the intensities of all feeding transitions taking into account the level scheme information presented in Fig. 3. The resulting  $\beta$ -feeding intensities are listed in the third column of Table II.

In order to estimate the character of the observed decays, the  $\beta$ -feeding intensities unfortunately are not sufficient since the decay of two different states, the  $11/2^-$  and the  $3/2^+$  states in  $^{129}\text{Cd}$ , is observed simultaneously. Since the half-lives of these two states are very similar, as discussed in the last section, the relative population of the two states in the present experiment cannot be estimated from the fit to the decay curve. Therefore, a different method had to be employed to estimate the number of decays originating from each of the two states. First, the intensity of the 2118 keV transition in  $^{129}\text{Sn}$ , populated in the daughter decay of the  $9/2^+$  ground state of  $^{129}\text{In}$ , was determined. Since the absolute intensity of this  $\gamma$  ray is known to be 42 (2) per 100 decays from the work of Gausemel *et al.* [16], it can be deduced from the observed intensity that 72 (2)% of all  $^{129}\text{Cd}$  decays end up in the  $9/2^+$  ground state of  $^{129}\text{In}$ . The remaining 28 (2)% are assigned to the  $1/2^-$  state. The absolute intensities of all  $\gamma$  rays populating the  $9/2^+$  state adds up to 61 (3)% which implies that 11 (3)% of all  $^{129}\text{Cd}$  decays proceed either directly to the  $9/2^+$  ground state, to states above 4 MeV which decay via weak high-energy  $\gamma$  rays below the detection limit of the current experiment or via  $\beta$ -delayed neutron emission. The equivalent number for the  $1/2^-$  state is 6 (3)%. Therefore, upper limits for the direct population of the  $9/2^+$  and  $1/2^-$  states of 14% and 9%, respectively, are deduced.

Still, this information is not sufficient to estimate the relative population of the two  $\beta$ -decaying states in  $^{129}\text{Cd}$  since it cannot be assumed that all decays from the  $11/2^-$  ( $3/2^+$ ) states in  $^{129}\text{Cd}$  end up in the  $9/2^+$  ( $1/2^-$ ) levels in  $^{129}\text{In}$ . To obtain the missing piece of information we use the same approach discussed already in the last section. There, a decay curve was constructed applying coincidence gates on the  $\gamma$

TABLE II. Excited states in  $^{129}\text{In}$  populated in the  $\beta$  decay of  $^{129}\text{Cd}$ , the total observed  $\beta$ -feeding intensities,  $I_{\beta^-}$ , the  $\beta$ -feeding intensities in the decay of either the  $3/2^+$  or  $11/2^-$  states,  $I_{\beta^-(3/2^+)}$  and  $I_{\beta^-(11/2^-)}$ , and the  $\log ft$  values for each decay.

$E_x$ (keV)	$I^\pi$	$I_{\beta^-}$ (%)	$I_{\beta^-(3/2^+)}$ (%)	$I_{\beta^-(11/2^-)}$ (%)	$\log ft$
0	$9/2^+$	<14		<28	>5.3
451	$1/2^-$	<9	<18		>5.4
995	$11/2^+$	6.5(20)		13(4)	5.4(1)
1083	$(3/2^-)$	3.6(6)	7(1)		5.7(1)
1220	$(5/2^-)$	3.0(17)	6(4)		5.7(6)
1354	$13/2^+$	3.2(12)		8(3)	5.5(2)
1555		<1.0	<2		>6.1
1621		1.2(4)	2(1)		6.1(2)
1688	$17/2^-$	<0.4		<1	>6.3
1693		0.7(6)		1(1)	6.3(5)
1762		0.5(10)	2(2)		6.0(5)
2015		1.1(3)		2(1)	5.9(2)
2060		1.3(6)	3(1)		5.8(2)
2085		<0.1		<1	>6.2
2088		<0.4	<1		>6.2
2143					
2217		1.4(6)		3(1)	5.7(2)
2433		<1.1	<2		>5.9
2447		1.3(11)	3(2)		5.7(3)
(2551)		<0.5		<1	>6.1
(2561)		<0.5		<1	>6.1
2589		<1.2		<2	>5.8
3150	$(13/2^-)$	25.3(8)		52(5)	4.2(1)
3184	$(5/2^+)$	13.3(8)	26(3)		4.5(1)
3286		0.4(1)	1(1)		5.9(5)
3348	$(5/2^+)$	8.6(9)	17(2)		4.7(1)
3488		0.7(2)	1(1)		5.8(5)
3702		1.6(6)	3(1)		5.3(2)
3888		1.2(4)	2(1)		5.4(2)
3914		0.9(2)	2(1)		5.4(2)
3966		1.9(4)	4(1)		5.1(1)
3971		0.7(1)			
4082		2.3(13)			
4118		1.0(3)	2(1)		5.3(2)

rays emitted in the decay of the ( $21/2^+$ ) ms isomer to the  $11/2^-$  state to select only decays from the  $11/2^-$  level. In the same way we now determine the intensities per 100 decays of the 995.1 and 1354.2 keV ground-state transitions in  $^{129}\text{In}$ . The result is that about 80 (16)% of all  $11/2^-$  decays proceed via one of these two transitions. Considering in addition the direct  $\beta$ -decay feeding to the  $9/2^+$  ground state, this information indicates that nearly all  $11/2^-$  decays proceed via the 995.1 and 1354.2 keV transitions or directly populate the  $9/2^+$  ground state. Consequently, the strongly populated states at 3184 and 3348 keV, whose decays mostly bypass the 995 keV state, have to be fed following the decay of the  $3/2^+$  state. Since most of the other states above the 3150 keV level show similar decay patterns to the 3184 and 3348 keV states, including a high-energy ground-state transition, it is very likely that they are populated in the  $3/2^+$  decay as well. Only the levels at

3971 and 4082 keV do not decay via ground-state transitions prohibiting their assignment to one or the other decaying state.

Assuming that only the 3150 keV state and the levels populated in its decay receive feeding from the  $11/2^-$  decay we can now finally determine the fraction of decays originating from each of the two  $\beta$ -decaying states in  $^{129}\text{Cd}$ . The sum of the absolute intensities of the 995.1 and 1354.2 keV transitions amounts to 40 (2)%, from which the intensity of the 1221.6 keV transition of 2 (1)% has to be subtracted and the “missing intensity” [11 (3)%, see above] added. We therefore conclude that 49 (4)% of all  $^{129}\text{Cd}$  decays proceed from the  $11/2^-$  state while the remaining 51 (4)% stem from the  $\beta$ -decaying  $3/2^+$  isomer. With this information, we can now calculate the  $\beta$  feeding from either of these states and finally the  $\log ft$  values for all transitions observed in the  $\beta$  decay of  $^{129}\text{Cd}$  taking into account the half-life values reported in the last section,  $Q_\beta = 9330$  (200) keV taken from Ref. [25] and assuming an excitation energy of the  $3/2^+$  state around 300 keV. The resulting  $\log ft$  values, calculated using LOGFT [26], are listed in the last column of Table II. Note that, as in all  $\beta$ -decay studies using high-resolution  $\gamma$ -ray spectroscopy, these  $\log ft$  values have, strictly speaking, to be considered as lower limits due to the pandemonium effect [27].

The states at 3150, 3184, and 3348 keV are populated with  $\log ft$  values of 4.2 (1), 4.5 (1), and 4.7 (1), respectively, clearly indicating a Gamow–Teller (GT) character of these decays. The GT transition dominating all known  $\beta$  decays in the region  $Z < 50$ ,  $N \leq 82$  is the  $\nu 0g_{7/2} \rightarrow \pi 0g_{9/2}$  decay. For example, GT transitions of this type are observed in the decay of the neighboring even Cd isotopes  $^{128,130}\text{Cd}$  with  $\log ft$  values of 4.2 (1) and 4.1, respectively [28,29]. In the decays of  $^{127,129}\text{In}$  slightly larger  $\log ft$  values in the range 4.4–4.5 were measured [16], while in the  $^{132}\text{In}$  decay a value of 4.6 was obtained [30].

For the 3150 keV level populated from the  $11/2^-$  state, the spin range is therefore limited to  $9/2^+$ ,  $11/2^+$ , and  $13/2^+$ . Considering that this state has direct decay branches to the  $11/2^+$ ,  $13/2^+$ , and  $17/2^-$  states, we tentatively propose a spin and parity of  $13/2^-$  for this state. For the states at 3184 and 3348 keV, which are strongly populated following the decay of the  $3/2^+$  state, values of  $1/2^+$ ,  $3/2^+$ , and  $5/2^+$  are possible based on the  $\log ft$  values. Considering the observation of decay branches to the  $9/2^+$  state, spin and parity of  $5/2^+$  is tentatively proposed for these two levels. All other states are fed with  $\log ft$  values in the range 5.1–6.3, suggesting that first-forbidden (ff) transitions may compete with GT decays.

### V. COMPARISON TO SHELL-MODEL CALCULATIONS AND DISCUSSION

Shell-model (SM) calculations for  $^{129}\text{In}$  were presented in Ref. [17]. Calculated energies of 1295, 1300, and 1540 keV were obtained for the  $11/2^+$ ,  $13/2^+$ , and  $17/2^-$  levels. A comparison to the experimental values of 995, 1354, and 1688 keV shows that the energy of the  $11/2^+$  state is calculated 300 keV too high while the ones of the other two states are slightly too low.

In Refs. [5,7] first results of SM calculations were presented which employ an empirically optimized two-body interaction

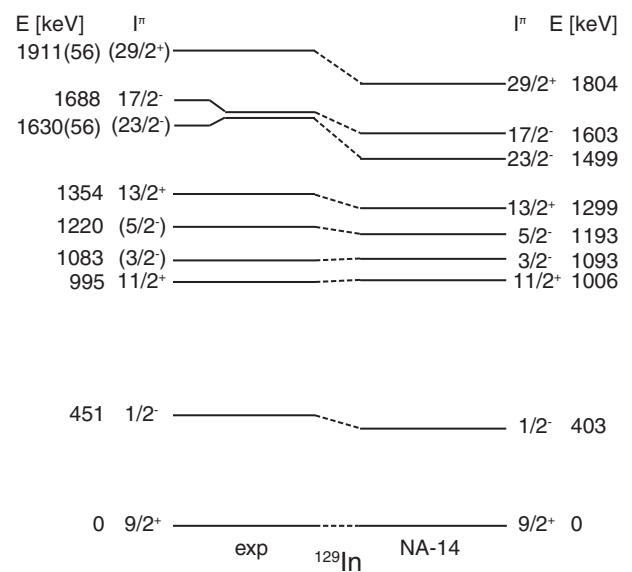


FIG. 7. Experimental and calculated energy levels in  $^{129}\text{In}$ . Only the experimental states below an excitation energy of 1.5 MeV and the known isomeric ( $23/2^-$ ),  $17/2^-$ , and ( $29/2^+$ ) states [15–17] are included in the comparison.

based on the one used in Ref. [17] and  $1p_{3/2}$  and  $1p_{1/2}$  proton single-hole energies from recent experimental work [7,14]. Here we use the same approach to calculate the spectrum of excited states in  $^{129}\text{In}$ . The two-body effective interaction is derived from the charge-dependent-Bonn (CD-Bonn) nucleon-nucleon potential renormalized by way of the  $V_{\text{low}k}$  approach. The multipole part of the interaction was modified as detailed in Refs. [5,7] yielding a consistent description of  $46 \leq Z \leq 50$ ,  $N \leq 82$  nuclei.

The nucleus  $^{132}\text{Sn}$  is used as a closed core and the full major  $Z = 28$  to 50 shell for proton holes (i.e., the orbitals  $0f_{5/2}$ ,  $1p_{3/2}$ ,  $1p_{1/2}$ , and  $0g_{9/2}$ ) and the full major  $N = 50$  to 82 shell for neutron holes (i.e., the orbitals  $0g_{7/2}$ ,  $1d_{5/2}$ ,  $1d_{3/2}$ ,  $2s_{1/2}$ , and  $0h_{11/2}$ ) are considered. All remaining single-hole energies are taken from Ref. [31] and the computer code OXBASH [32] was used to perform the calculations. The GT transitions were calculated by assuming a general quenching factor of 0.75 for the GT matrix element as established for the  $N = 1, 2, 3$  harmonic-oscillator shells [33] and for  $N = 4$  in the  $^{100}\text{Sn} \beta^+/\text{EC}$  decay [34].

Figure 7 shows a comparison between the experimentally established excited states in  $^{129}\text{In}$  below 1.5 MeV and the SM predictions. Above this energy the level density of both experimental and calculated states increases, impeding the identification of one-to-one correlations between the two sets of states. Above 1.5 MeV we only include the three known isomeric states for which, at least tentative, spin assignments are available. In general a very good agreement is found between the calculated and measured energies. In particular, the energies of the  $11/2^+$ ,  $13/2^+$ , and  $17/2^-$  levels are much better reproduced as compared to the SM calculation reported in Ref. [17].

Our shell-model calculations confirm the assignment of the  $\pi g_{9/2}^{-1} \nu (d_{3/2}^{-1} h_{11/2}^{-1})$  configuration to the isomeric  $17/2^-$  state. Due to its high spin this state is not expected to receive any

measurable  $\beta$  feeding from either the  $11/2^-$  or the  $3/2^+$   $\beta$ -decaying states in  $^{129}\text{Cd}$ , in agreement with the experimental findings. In contrast we observe non-negligible feeding to the  $11/2^+$  and  $13/2^+$  levels at 995 and 1354 keV, for which the SM calculations indicate the  $\pi g_{9/2}^{-1}\nu h_{11/2}^{-2}$  configuration. These states are most likely populated via the ff transition  $\nu 0h_{11/2} \rightarrow \pi 0g_{9/2}$  from the  $11/2^-$  state in  $^{129}\text{Cd}$ . The corresponding  $\log ft$  values are 5.4 (1) and 5.5 (2). The same decay proceeds also to the  $9/2^+$  ground state with  $\log ft > 5.3$ . A slightly larger value of  $\log ft = 5.7$  was reported for a ff transition of the same type in the decay of  $^{132}\text{In}$  [30].

Turning now to the low-spin negative-parity states, for the  $1/2^-$  level an excitation energy of 403 keV is obtained in the shell-model calculation, in rather good agreement with the experimental value of 451 keV. The excited states at 1083 and 1220 keV, both showing a strong decay branch to the  $1/2^-$  level, most probably correspond to the  $3/2^-$  and  $5/2^-$  states, predicted at energies of 1093 and 1193 keV in the calculations. These three negative-parity states are all directly populated in the  $\beta$  decay of the  $3/2^+$  state with  $\log ft$  values  $> 5.4$ , 5.7 (1), and 5.7 (6), respectively. It is likely that these decays are driven by ff transitions of the type  $\nu d_{3/2} \rightarrow \pi(p, f_{5/2})$ .

Finally, note that the energies of the two ms high-spin isomers [15,16], which are not observed in the present work, are also rather well reproduced by the present SM calculations. The energies of these states with spin and parity of  $(29/2^+)$  and  $(23/2^-)$ , which represent the fully aligned  $\pi g_{9/2}^{-1}\nu h_{11/2}^{-2}$  and  $\pi g_{9/2}^{-1}\nu(d_{3/2}^{-1}h_{11/2}^{-1})$  configurations, respectively, are only slightly underestimated beyond their experimental uncertainty by the calculations.

Let us consider now the high-lying excited states in  $^{129}\text{In}$  which are strongly populated in the GT decay of the  $11/2^-$  and  $3/2^+$  states in  $^{129}\text{Cd}$ . As discussed in the last section, spin and parity values of  $(13/2^-)$ ,  $(5/2^+)$ , and  $(5/2^+)$  were tentatively assigned to the states with excitation energies of 3150, 3184, and 3348 keV based on the experimental  $\log ft$  values and  $\gamma$ -decay branches. Since the  $\nu 0g_{7/2} \rightarrow \pi 0g_{9/2}$  GT single-particle transition is the only GT decay which populates excited states in  $^{129}\text{In}$  below the neutron separation energy of  $S_n = 6760$  (150) keV [25], configurations of  $\pi g_{9/2}^{-1}\nu(g_{7/2}^{-1}h_{11/2}^{-1})$  and  $\pi g_{9/2}^{-1}\nu(g_{7/2}^{-1}d_{3/2}^{-1})$  can be assigned to the  $(13/2^-)$  and  $(5/2^+)$  states, respectively. In the SM calculations, a number of  $13/2^-$  and  $5/2^+$  states are obtained in the excitation energy range 3–4 MeV. The calculated GT distributions for the decay of the  $11/2^-$  and  $3/2^+$  states in  $^{129}\text{Cd}$  are shown in Fig. 8. The strongest decay branch from the  $11/2^-$  state populates the fifth calculated  $13/2^-$  state at an excitation energy of 3137 keV, in good agreement with the position of the experimentally observed  $(13/2^-)$  state at 3150 keV. The wave function of this calculated  $13/2^-$  state indeed comprises a 92% partition of the  $\pi g_{9/2}^{-1}\nu(g_{7/2}^{-1}h_{11/2}^{-1})$  configuration. With respect to the decay of the  $3/2^+$  state, the GT resonance is calculated at slightly higher excitation energies in the shell model as compared to the experimental findings (see Fig. 8). However, the calculation nicely reproduces the experimentally observed stronger fragmentation of the GT strength in the decay of the  $3/2^+$  as compared to that of the  $11/2^-$  state. We consider it a remarkable feature of the present shell-model calculations that

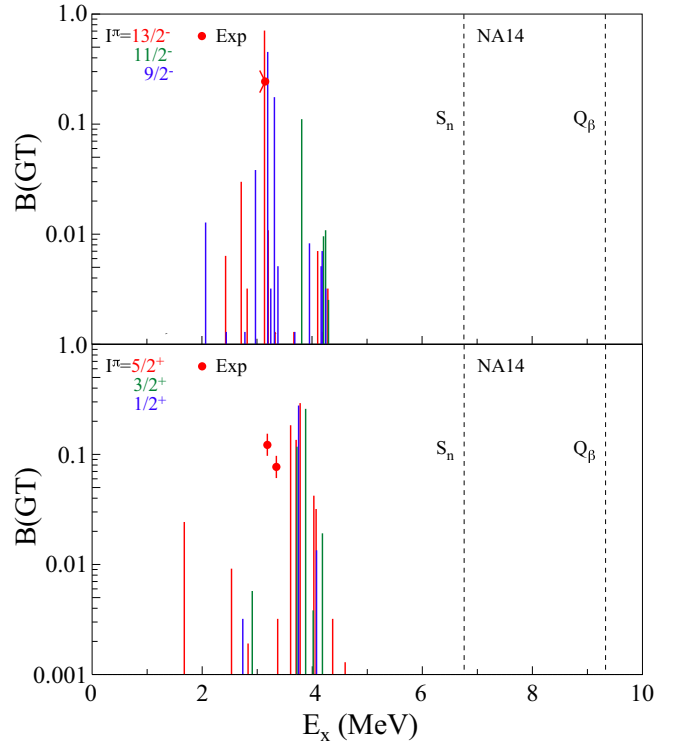


FIG. 8. (Color online) Distribution of the GT strengths,  $B(\text{GT})$ , for the decay of the  $11/2^-$  (top) and  $3/2^+$  (bottom) states in  $^{129}\text{Cd}$  as obtained within the present shell-model approach. The experimental GT strengths to the  $(13/2^-)$  state at an excitation energy of 3150 keV and the  $(5/2^+)$  levels at 3184 and 3348 keV are shown as red dots with error bars.

they not only describe the energies of the low-lying yrast states (see Fig. 7) but that, at the same time, also highly non-yrast states are satisfactorily reproduced. The overestimation of the absolute strength in Fig. 8 is due to the fact that the present model space does not include the full  $N = 4$  shell for protons.

Ultimately we would like to note that the comparable decay pattern of the  $11/2^-$  and  $3/2^+$  levels may explain the experimentally established similarity of the half-lives of these two states. Both the  $\nu 0g_{7/2} \rightarrow \pi 0g_{9/2}$  GT as well as the first forbidden decays from the two beta-decaying states populate levels in the same excitation energy range in  $^{129}\text{In}$ .

## VI. CONCLUSIONS

We reported on a study of the  $\beta$  decay of  $^{129}\text{Cd}$ . The half-lives of the two  $\beta$ -decaying states, with spin and parity of  $11/2^-$  and  $3/2^+$ , were measured and found to be rather similar, in disagreement with literature values. As in most  $\beta$  decays in the  $Z < 50$ ,  $N \leq 82$  region, the  $\nu 0g_{7/2} \rightarrow \pi 0g_{9/2}$  GT decay was found to dominate the  $\beta$  decay of  $^{129}\text{Cd}$ . However, a considerable fraction of the decays of the  $11/2^-$  state proceed via the ff transition  $\nu 0h_{11/2} \rightarrow \pi 0g_{9/2}$ , populating the  $(9/2^+)$  ground state as well as the  $11/2^+$  and  $13/2^+$  members of the  $\pi g_{9/2}^{-1}\nu h_{11/2}^{-2}$  multiplet. Also, in the decay of the  $3/2^+$  state, branches to the  $1/2^-$ ,  $(3/2^-)$ , and  $(5/2^-)$  states were identified which correspond to ff decays. These findings suggest once more that ff transitions can provide

non-negligible contributions to the  $\beta$ -decay half-lives in this region.

Furthermore, a very detailed level scheme of  $^{129}\text{In}$  was established including 31 excited states connected by 69  $\gamma$ -rays in the energy range from 137 to 4118 keV. The excitation energies of the low-lying and isomeric states in  $^{129}\text{In}$  were compared to shell-model calculations performed employing a new interaction and the experimental energy of the  $p_{3/2}$  proton-hole state recently reported in Ref. [7]. A good agreement was found between calculated and experimental excitation energies.

#### ACKNOWLEDGMENTS

We thank the staff of the RIKEN Nishina Center accelerator complex for providing us very stable beams throughout the experiment with high intensities. We acknowledge the

EUROBALL Owners Committee for the loan of germanium detectors and the PreSpec Collaboration for the readout electronics of the cluster detectors. This work was supported by the Spanish Ministerio de Ciencia e Innovación under contracts FPA2009-13377-C02 and FPA2011-29854-C04, the Generalitat Valenciana (Spain) under grant PROMETEO/2010/101, the National Research Foundation of Korea (NRF) grant funded by the Korea government (MEST) (No. NRF-2012R1A1A1041763), the Priority Centers Research Program in Korea (2009-0093817), OTKA contract number K-100835, JSPS KAKENHI (Grant No. 25247045), the European Commission through the Marie Curie Actions call FP7-PEOPLE-2011-IEF under Contract No. 300096, the US Department of Energy, Office of Nuclear Physics, under Contract No. DE-AC02-06CH11357, the “RIKEN foreign research program,” and the German BMBF (No. 05P12RDCIA and 05P12RDNUP) and HIC for FAIR.

- 
- [1] G. Lorusso *et al.*, *Phys. Rev. Lett.* **114**, 192501 (2015).  
[2] P. Möller, B. Pfeiffer, and K.-L. Kratz, *Phys. Rev. C* **67**, 055802 (2003).  
[3] I. Borzov, J. Cuenca-García, K. Langanke, G. Martínez-Pinedo, and F. Montes, *Nucl. Phys. A* **814**, 159 (2008).  
[4] I. N. Borzov, *Phys. Rev. C* **67**, 025802 (2003).  
[5] J. Taprogge *et al.*, *Phys. Lett. B* **738**, 223 (2014).  
[6] G. S. Simpson *et al.*, *Phys. Rev. Lett.* **113**, 132502 (2014).  
[7] J. Taprogge *et al.*, *Phys. Rev. Lett.* **112**, 132501 (2014); **113**, 049902 (2014).  
[8] O. Arndt, Diploma thesis, Universität Mainz, 2003 (unpublished).  
[9] O. Arndt *et al.*, *Annual Reports of the Institute for Nuclear Chemistry* (University of Mainz, Germany, 2003), p. A15.  
[10] K.-L. Kratz *et al.*, *Eur. Phys. J. A* **25**, 633 (2005).  
[11] O. Arndt *et al.*, *Acta Phys. Pol. B* **40**, 437 (2009).  
[12] D. T. Yordanov *et al.*, *Phys. Rev. Lett.* **110**, 192501 (2013).  
[13] L. E. De Geer and G. B. Holm, *Phys. Rev. C* **22**, 2163 (1980).  
[14] A. Kankainen *et al.*, *Phys. Rev. C* **87**, 024307 (2013).  
[15] B. Fogelberg, H. Mach, H. Gausemel, J. P. Omtved, and K. A. Mezilev, Nuclear Fission and Fission-Product Spectroscopy, AIP Conf. Proc. No. 447 (AIP, Melville, 1998), p. 191.  
[16] H. Gausemel *et al.*, *Phys. Rev. C* **69**, 054307 (2004).  
[17] J. Genevey *et al.*, *Phys. Rev. C* **67**, 054312 (2003).  
[18] I. Dillmann *et al.*, *Annual Reports of the Institute for Nuclear Chemistry* (University of Mainz, Germany, 2003), p. A14.  
[19] T. Kubo *et al.*, *Prog. Theor. Exp. Phys.* **2012**, 03C003 (2012).  
[20] N. Fukuda *et al.*, *Nucl. Instrum. Methods Phys. Res., Sect. B* **317**, 323 (2013).  
[21] S. Nishimura *et al.*, RIKEN Accel. Progr. Rep. **46**, 182 (2013).  
[22] P.-A. Söderström *et al.*, *Nucl. Instrum. Methods Phys. Res., Sect. B* **317**, 649 (2013).  
[23] J. Eberth *et al.*, *Prog. Part. Nucl. Phys.* **28**, 495 (1992).  
[24] <http://www.nndc.bnl.gov/ensdf/>.  
[25] M. Wang *et al.*, *Chin. Phys. C* **36**, 1603 (2012).  
[26] <http://www.nndc.bnl.gov/logft/>.  
[27] J. Hardy, L. Carraz, B. Jonson, and P. Hansen, *Phys. Lett. B* **71**, 307 (1977).  
[28] B. Fogelberg, in *Proc. Intern. Conf. Nuclear Data for Science and Technology, Mito, Japan*, edited by S. Igarasi (Japanese Atomic Energy Research Institute, 1988), p. 827.  
[29] I. Dillmann *et al.*, *Phys. Rev. Lett.* **91**, 162503 (2003).  
[30] B. Fogelberg *et al.*, *Phys. Rev. Lett.* **73**, 2413 (1994).  
[31] H. Grawe, K. Langanke, and G. Martínez-Pinedo, *Rep. Prog. Phys.* **70**, 1525 (2007).  
[32] B. A. Brown *et al.*, MSU-NSCL report 1289 (2009).  
[33] E. Caurier *et al.*, *Rev. Mod. Phys.* **77**, 427 (2005).  
[34] C. B. Hinke *et al.*, *Nature (London)* **486**, 341 (2012).